ELSEVIER

Mechanisms of Development 57 (1996) 145–157

Overexpression of BMP-2 and BMP-4 alters the size and shape of developing skeletal elements in the chick limb

Delphine Duprez[a], Esther J. de H. Bell[a,b], Michael K. Richardson[b,1], Charles W. Archer[c], Lewis Wolpert[b,*], Paul M. Brickell[a], Philippa H. Francis-West[a,b,2]

[a]*The Medical Molecular Biology Unit, Department of Molecular Pathology, University College London Medical School, The Windeyer Building, Cleveland Street, London WIP 6DB, UK*

[b]*Department of Anatomy and Developmental Biology, University College London Medical School, The Windeyer Building, Cleveland Street, London WIP 6DB, UK*

[c]*School of Molecular and Medical Biosciences, University of Wales, Cardiff CF1 3YF, UK*

Received 27 February 1996; revision received 9 April 1996; accepted 9 April 1996

Abstract

Bone morphogenetic proteins are members of the transforming growth factor β (TGFβ) superfamily which are involved in a range of developmental processes including modelling of the skeleton. We show here that *Bmp-2* is expressed in mesenchyme surrounding early cartilage condensations in the developing chick limb, and that *Bmp-4* is expressed in the perichondrium of developing cartilage elements. To investigate their roles during cartilage development, BMP-2 and BMP-4 were expressed ectopically in developing chick limbs using retroviral vectors. Over-expression of BMP-2 or BMP-4 led to a dramatic increase in the volume of cartilage elements, altered their shapes and led to joint fusions. This increase in volume appeared to result from an increase in the amount of matrix and in the number of chondrocytes. The latter did not appear to be due to increased proliferation of chondrocytes, suggesting that it may result from increased recruitment of precursors. BMP-2 and BMP-4 also delayed hypertrophy of chondrocytes and formation of the osteogenic periosteum. These data provide insights into how BMP-2 and BMP-4 may model and control the growth of skeletal elements during normal embryonic development, suggesting roles for both molecules in recruiting non-chondrogenic precursors to chondrogenic fate.

Keywords: Limb; Cartilage; Chondrocytes; BMP-2; BMP-4; Retrovirus; Perichondrium

1. Introduction

The formation of skeletal elements with the correct shape during embryonic development is a fundamental problem and precise morphogenesis is a pre-requisite for a functional skeleton. However, the signals involved in determining the size and shape of cartilage elements are relatively unknown (Thorogood, 1983; Wolpert and Tickle, 1993). Several members of the transforming growth factor β (TGFβ) superfamily affect cartilage differentiation and morphogenesis, including members of the Bone Morphogenetic Protein (BMP) and Growth/ Differentiation Factor (GDF) families. For example, in mice, mutation in *Bmp-5* affects development of the ears, sternum and certain ribs (Kingsley et al., 1992), whilst mutation in *Gdf-5* results in shortened appendicular elements and irregularly shaped tarsals but has no effect on the axial skeleton (Storm et al., 1994). Consequently, it has been proposed that each skeletal element requires a specific repertoire of TGFβ superfamily members for normal morphogenesis (Kingsley, 1994; Storm et al., 1994).

The characteristic pattern of cartilage elements in the limb arises from an outgrowth of undifferentiated mesenchyme. The cartilage elements initially appear as dense condensations of cells which differentiate into chondrocytes (reviewed by Thorogood, 1983; Rooney et al., 1984). The chondrocytes then secrete matrix and subsequently undergo

* Corresponding author. Tel.: +44 171 3809345; fax: +44 171 3809346.

[1] Current address: Department of Anatomy, St. George's Hospital Medical School, Cranmer Terrace, London SW17 ORE, UK.

[2] Current address: Department of Craniofacial Development, UMDS, Floor 28, Guy's Tower, London Bridge, London SE1 9RT, UK.

0925-4773/96/$15.00
PII: S0925-4773(96)00540-0

hypertrophy, becoming organised into distinct zones of hypertrophic, flattened and rounded chondrocytes. Cells at the periphery of the condensation become orientated longitudinally to form a perichondrium which is thought to act as a constraining sheath facilitating the expansion of the cartilage along the long axis (Rooney and Archer, 1992). The perichondrium may also contribute to appositional growth of the cartilage (Fell and Canti, 1934). At later stages of development, the perichondrium gives rise to the periosteum, which is the source of osteogenic precursors (Rooney and Archer, 1992). The signals that determine growth, cell orientation and differentiation of chondrocytes are unknown.

In situ hybridisation studies have suggested that expression of different *Bmp* genes is associated with distinct differentiative and morphogenetic events. For example, in mice, *Bmp-2* and *Bmp-5* are expressed in the initial cartilage condensation (Lyons et al., 1989; Wozney et al., 1993), *Bmp-3* and *Bmp-6* (also known as Vgr-1) are expressed in hypertrophic chondrocytes, and *Bmp-4* is expressed in the perichondrium (Wozney et al., 1993). In addition, *Gdf-5* expression has been localised to chondrocytes, the perichondrium and the joint interzone of the appendicular skeleton (Chang et al., 1994; Storm et al., 1994). These different expression patterns suggest that different family members play distinct roles during cartilage differentiation and morphogenesis. Consistent with this idea, in vitro studies have suggested that members of the TGFβ family may act sequentially during cartilage differentiation (Chen et al., 1991; Roark and Greer, 1994).

To investigate the roles of BMP-2 and BMP-4 during skeletal growth and morphogenesis, we over-expressed BMP-2 and BMP-4 during chick limb development using avian retroviral vectors. The results suggest that BMP-2 and/or BMP-4 may be involved in determining the size and shape of skeletal elements during limb development.

2. Results

2.1. Expression of Bmp-2 and Bmp-4 in developing skeletal elements

We have previously shown that during early limb development and prior to the onset of overt chondrogenesis, *Bmp-2* is expressed in posterior mesenchyme and apical ectodermal ridge, whilst *Bmp-4* is expressed in mesenchyme at the margins of the limb bud and in apical ectodermal ridge (Francis et al., 1994). During later development, at stage 27, *Bmp-2* is expressed in mesenchyme surrounding early cartilage condensations, as well as in mesenchyme at the margins of the developing limb (Fig. 1A). *Bmp-4* is not expressed in regions of early cartilage condensations at this stage (data not shown), but by stage 30 is

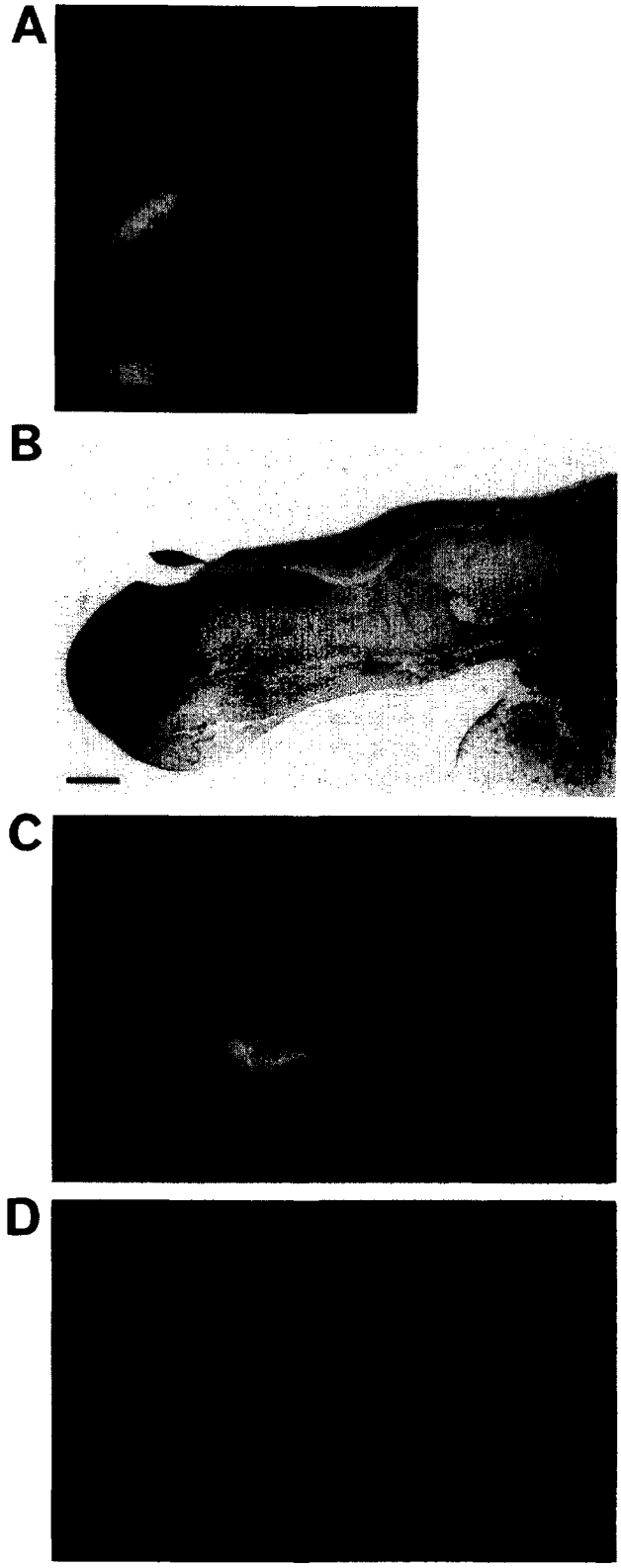

Fig. 1. (A) Longitudinal section through a stage 27 chick wing, hybridised with a ^{35}S-labelled antisense RNA probe specific for chicken *Bmp-2* transcripts and photographed under dark-field illumination. (B,C) Longitudinal section through a stage 30 chick wing, hybridised with a ^{35}S-labelled antisense RNA probe specific for chicken *Bmp-4* transcripts and photographed under bright-field (B) or dark-field (C) illumination. Perichondrium is arrowed. (D) Section adjacent to (B,C), hybridised with a negative control sense RNA probe and photographed under dark-field illumination. Scale bars = 100 μm.

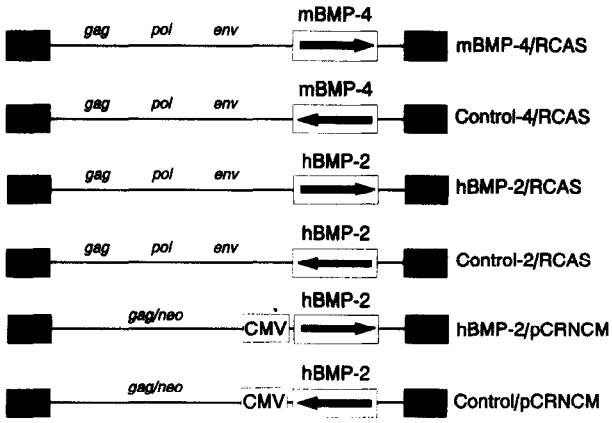

Fig. 2. Structures of the proviral forms of retroviral constructs. Viral long terminal repeats are shown as black boxes. Arrows show the orientation of BMP coding regions, with respect to the upstream promoter. CMV, cytomegalovirus immediate early gene promoter.

expressed in the perichondrium of the cartilage elements, as well as in mesenchyme at the margin of the developing limb (Fig. 1B–D).

2.2. Construction and testing of retroviruses

To examine roles of BMP-2 and BMP-4 during skeletal morphogenesis, cDNA sequences encoding human BMP-2 (hBMP-2) or mouse BMP-4 (mBMP-4) were inserted into replication-competent retrovirus RCASBP(A) in the sense orientation (hBMP-2/RCAS and mBMP-4/RCAS) or, as negative controls, in the antisense orientation (Control-2/RCAS and Control-4/RCAS) (Fig. 2). The hBMP-2 coding region was also inserted into replication-defective retroviral vector pCRNCM, yielding hBMP-2/pCRNCM (insert in the sense orientation) and Control/pCRNCM (insert in the antisense orientation) (Fig. 2). In pCRNCM-based viruses, the insert is transcribed from an internal CMV immediate early gene promoter (Fig. 2). In RCAS-based viruses, the insert is transcribed as part of a full-length primary viral transcript originating in the upstream LTR (Fig. 2), and efficient expression of inserted sequences requires efficient splicing of this primary viral transcript. Northern hybridization showed that chicken cells spliced primary viral transcripts efficiently to produce BMP mRNA (data not shown).

We chose to use human *Bmp-2* and mouse *Bmp-4* sequences in the viruses as this would allow us to distinguish viral transcripts from endogenous chicken *Bmp-2* and *Bmp-4* transcripts in infected embryos, using species-specific probes. Human BMP-2 shares 94% amino acid sequence identity with chicken BMP-2 in the functional C-terminal domain, while mouse BMP-4 shares 98% amino acid sequence identity with chicken BMP-4 in this region (Francis et al., 1994). To test that the viruses directed expression of functional human BMP-2 or mouse BMP-4 that was active on chicken cells, we added supernatants from mBMP-4/RCAS-infected CEF, hBMP-2/RCAS-infected CEF or hBMP-2/pCRNCM-infected Q2bn cells to micromass cultures of stage 21 chick limb bud mesenchyme cells. All three viral supernatants stimulated cartilage formation (data not shown). This is consistent with previous reports in which recombinant BMP-2 and BMP-4 were shown to increase chondrogenesis in such cultures (Chen et al., 1992; Roark and Greer, 1994). Supernatants from cells infected with the three negative control viruses had no effect on micromass cultures.

2.3. Gross morphology of limbs infected with replication-competent RCAS-based viruses

Pellets of CEF infected with hBMP-2/RCAS, mBMP-4/RCAS, Control-2/RCAS or Control-4/RCAS virus were grafted to chick limb buds at various stages of development. Since the viruses were replication-competent, they spread through infected tissue. The extent of viral spread was determined by in situ hybridisation to whole embryos using species-specific probes for h*Bmp-2* or m*Bmp-4* transcripts. This allowed us to correlate limb phenotype with virus spread. It should be noted that the probes do not distinguish between spliced and unspliced viral transcripts when used for in situ hybridization.

Grafting of hBMP-2/RCAS-infected CEF ($n = 18$) or hBMP-4/RCAS-infected CEF ($n = 27$) to the wing bud between stages 17 and 26, resulted in formation of thickened, abnormally shaped cartilage elements which were often fused at the joint region (Figs. 3 and 4). The volume of affected elements was up to five-fold greater than that of normal elements. The most severe effects were observed by grafting virus-infected CEF into early limb buds at stages 17–22 (BMP-2, $n = 13$; BMP-4, $n = 18$). In all of these cases, the majority of the skeletal elements were affected, with some skeletal elements exhibiting marked dysplasia and joint fusion. In some of these cases (BMP-2, $n = 5$; BMP-4, $n = 3$), every skeletal element of the limb, including the scapula, was thickened and deformed (Figs. 3B and 4C). In contrast, grafting into older limb buds at stages 23–26 (BMP-2, $n = 5$; BMP-4, $n = 9$), resulted in marked thickening of one or two elements, particularly in the epiphyseal regions, but joints were not fused and the diaphyseal regions appeared normal (Figs. 3C,D and 4E). Grafting of infected CEF into the proximal part of the limb bud at stages 27–29, after cartilage elements had been established, did not affect cartilage development, but in these limbs virus spread was limited (BMP-2, $n = 5$; BMP-4, $n = 6$).

Control grafts of CEF infected with Control-2/RCAS virus ($n = 15$) or Control-4/RCAS virus ($n = 13$) resulted in development of normal limbs, with no thickening of cartilage elements. Control viruses spread through infected wing buds to the same extent as hBMP-2/RCAS and mBMP-4/RCAS (data not shown).

To correlate viral spread with skeletal phenotype in more detail, severely malformed limbs ($n = 2$) and partially affected limbs ($n = 2$) were sectioned and probed for

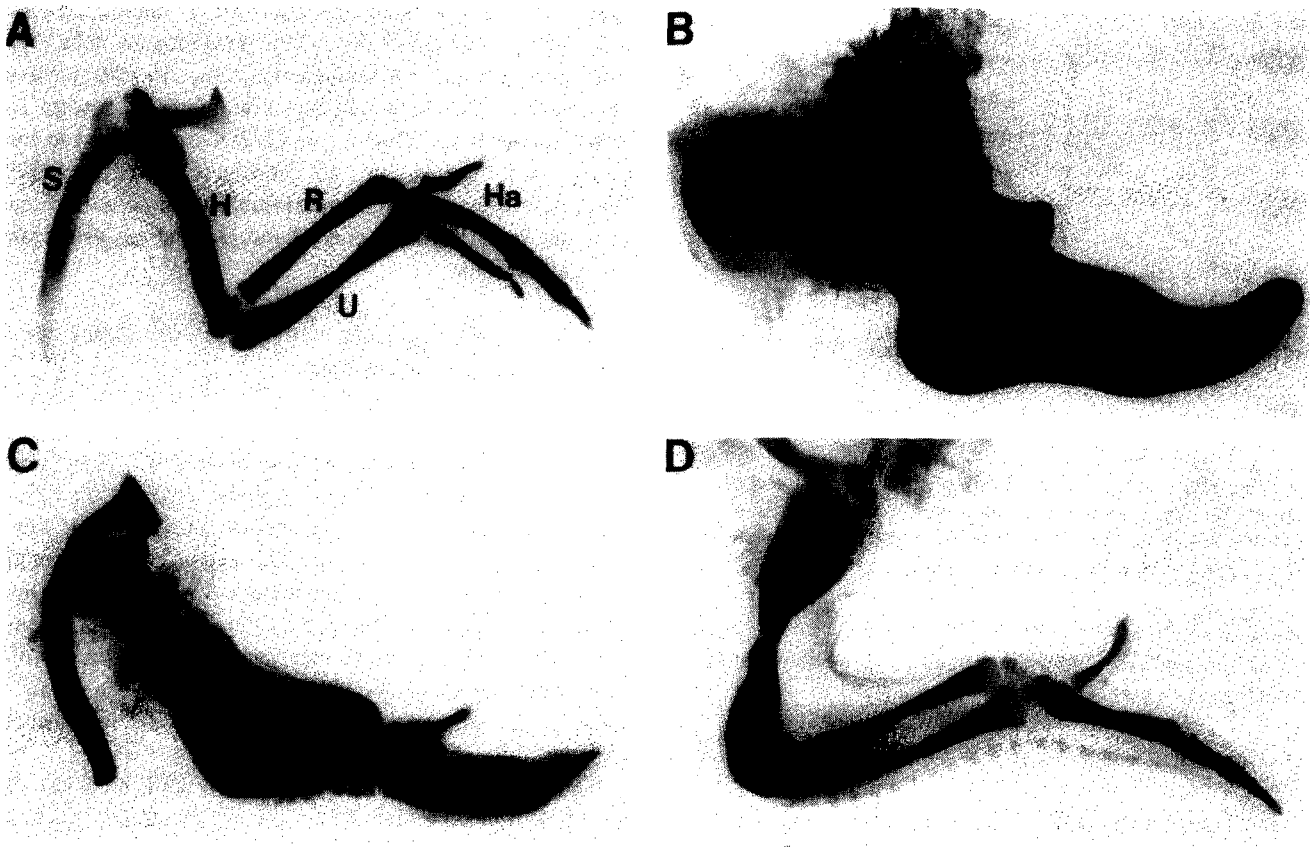

Fig. 3. Comparison of skeletal elements in control wings (A) and mBMP-4/RCAS-infected wings (B–D). CEF infected with mBMP-4/RCAS were grafted mid-proximally into the right wing bud of stage 19 (B), stage 21 (C), and stage 23 (D) chick embryos. In (B), all cartilage elements, including the scapula, are thickened. The elements are fused. In (C), the ulna is affected and is mis-shapen. The humerus is enlarged at its distal end. In (D), the humerus is thickened at the epiphyses. H, humerus; Ha, hand; R, radius; S, scapula , U, ulna. Scale bar = 1 mm.

m*Bmp-4* transcripts. In severely affected limbs, virus was present in all tissues including chondrocytes, and was present throughout the limb bud (Fig. 4C,D). However, in partially affected limbs, virus spread was not as extensive (Fig. 4E,F). Viral transcripts were again present in all tissues including muscle, loose connective tissue and cartilage elements (Fig. 4F).

2.4. *Gross morphology of limbs infected with replication-defective pCRNCM-based viruses*

To further examine the relationship between presence of virus and malformation of cartilage elements, we grafted Q2bn cells infected with replication-defective hBMP-2/pCRNCM virus to different parts of the developing limb, at stages just before the appearance of pre-cartilage condensations. In situ hybridization to h*Bmp-2* transcripts in whole mount preparations showed that virus remained localized to the region of grafted cells, 10 h and 48 h after grafting (Fig. 5).

When Q2bn cells infected with hBMP-2/pCRNCM were grafted to the proximal region of the limb bud at stage 21/22, in the position of presumptive humerus (Saunders, 1948; Bowen et al., 1989), the humerus was shortened and thickened in 75% of cases, but radius/ulna and digits were unaffected (Fig. 6A,B; $n = 8$). In contrast, grafting to the central region of the limb bud at stage 21/22, in the position of presumptive radius/ulna (Saunders, 1948; Bowen et al., 1989), resulted in shortening and thickening of the radius and ulna in 76% of cases (Fig. 6C,D; $n = 25$). In two of these cases the humerus was also shortened and thickened, an effect that correlated with the position of the graft. Digits were not affected. Similar effects on the radius/ulna could be obtained when virus-infected cells were grafted at stage 24 ($n = 4$), but no effects were seen when virus-infected cells were grafted at stage 26 or later ($n = 10$). When Q2bn cells infected with Control/pCRNCM virus were grafted to stage 21/22 limb buds, there was no effect on limb development, wherever grafts were placed ($n = 10$).

2.5. *Histological and immunocytochemical analysis of affected limbs*

To determine possible mechanisms by which ectopically expressed hBMP-2 and mBMP-4 cause an increase in the volume of cartilage elements, hBMP-2/RCAS- and mBMP-4-infected limbs and normal contralateral limbs were examined histologically. In normal cartilage elements, chondro-

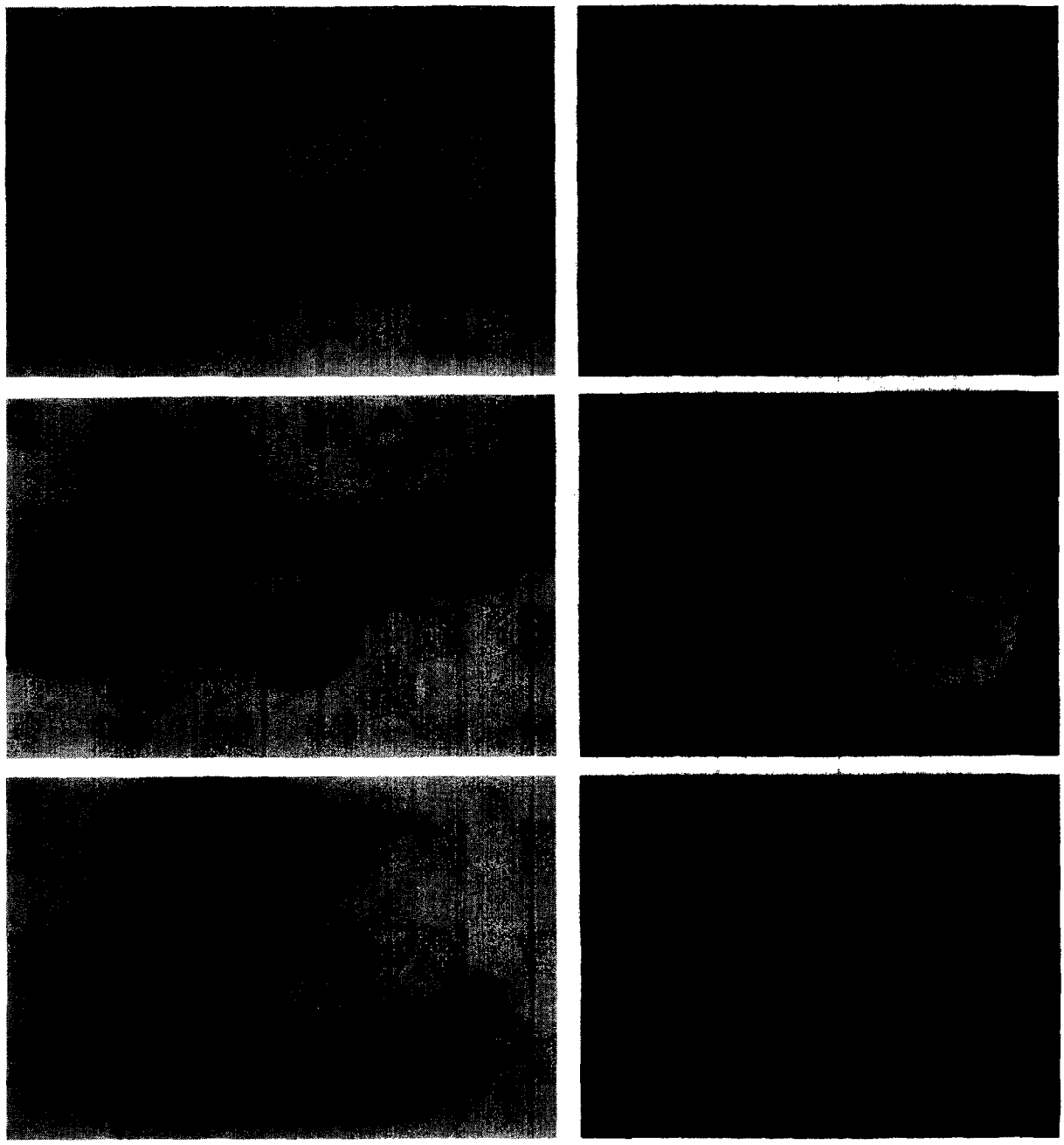

Fig. 4. Longitudinal sections through control and mBMP-4/RCAS-infected 10 day chick embryo limbs to show the morphology of cartilage elements and the extent of viral spread. (A,B) Control limbs. (C,D) Grossly affected limbs. (E,F) Partially affected limbs in which the humerus was thickened. Sections (A,C,E) were stained with Mallory's triple stain. Sections (B,D,F) were probed for mouse *Bmp-4* transcripts. Autoradiographic signal is seen as white staining under dark-field illumination. d, digits; h, humerus; r, radius; s, scapula; u, ulna. Scale bar = 1875 μm.

cytes are arranged in distinct zones with hypertrophic chondrocytes in the diaphyseal region, rounded cells at the epiphyses and flattened chondrocytes situated between these two cell types in the metaphyseal region (Fig. 7A–C). In partially affected elements, there was a normal arrangement of chondrocyte cell types, and normal subperiosteal osteogenesis, but the epiphyseal regions were broader (Figs. 3D and 4E, and data not shown). By contrast, in severely affected elements, characteristic zones of chondrocytes were not apparent and the size and shape of the cells had changed. Most cells were rounded, and there were occasional flattened cells (Fig. 7D–F). Chondrocytes in the epiphyseal region of control elements were smaller than those in comparable regions of severely affected elements (compare Fig. 7A and Fig. 7D). In these severely affected limbs, the diaphyseal chondrocytes did not appear to have undergone hypertrophy and there was little evidence of distinct lacunae (compare Fig. 7C and Fig. 7F). This impression was tested by performing immunocytochemistry for type X collagen, which is a marker of

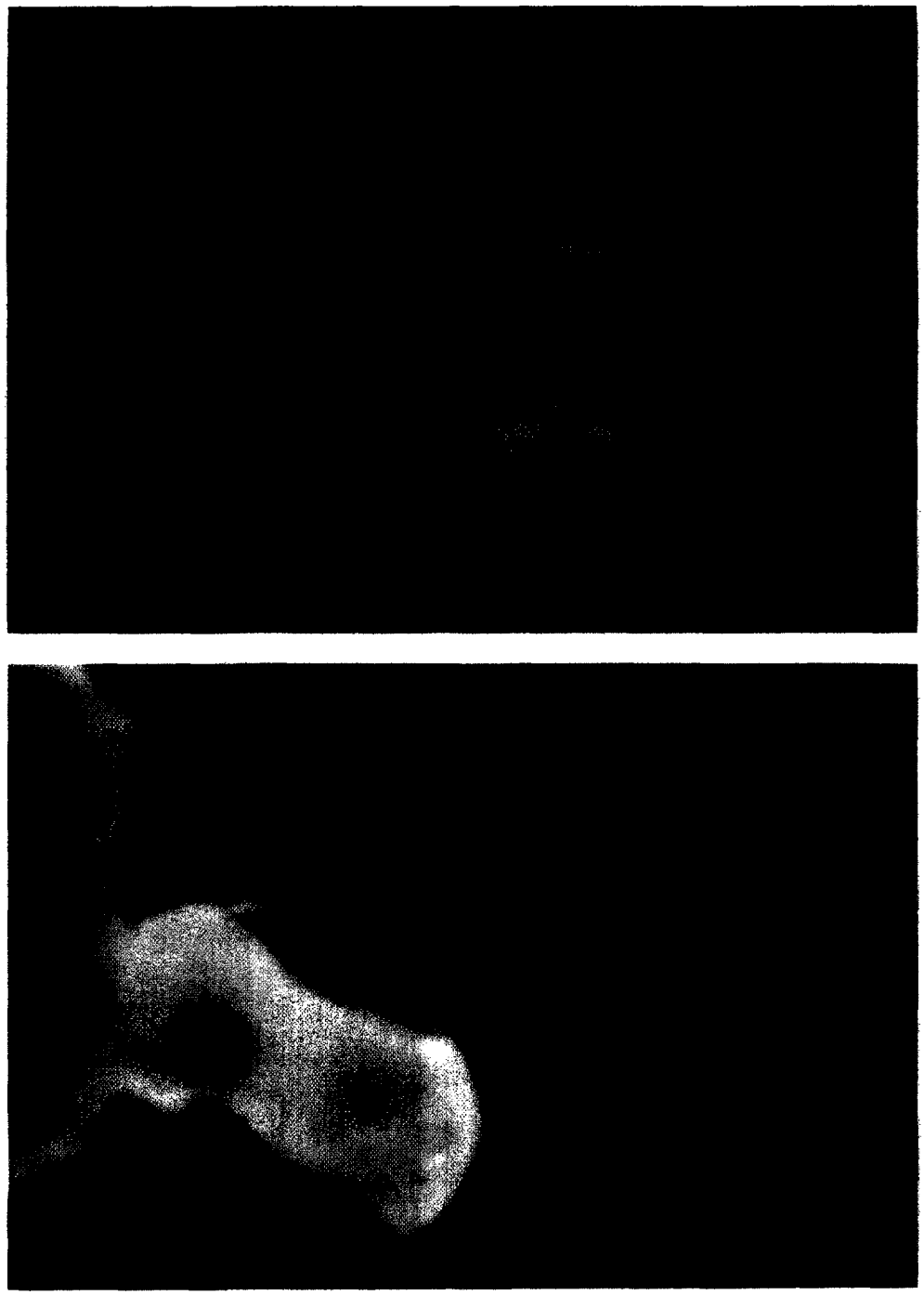

Fig. 5. Distribution of replication-defective hBMP-2/pCRNCM virus in whole mount preparations of limbs grafted centrally at stage 21/22 with hBMP-2/pCRNCM-infected Q2bn cells. Virus was detected 10 h (A) or 48 h (B) after grafting by in situ hybridization to human *Bmp-2* transcripts, and is stained purple. Scale bar = 375 μm.

hypertrophic chondrocytes. Humeral diaphyseal regions of control limbs were immunopositive for type X collagen (Fig. 8A), but the protein was undetectable in any region of affected limbs (Fig. 8B).

We also examined the chondrial/periosteal structure in affected elements (Fig. 9). In some regions surrounding affected elements, a perichondrial structure was either not apparent or, if present, appeared to be undergoing chondro-

Fig. 6. Effects of grafting hBMP-2/pCRNCM-infected Q2bn cells to different regions of presumptive cartilage at stage 21/22. Whole mount preparations were stained with alcian green on embryonic day 10. When grafts were placed proximally (A), in the region of presumptive humerus, the wing had a shortened, thickened humerus (B). When grafts were placed more distally (C), in the region of presumptive radius/ulna, the radius/ulna were shortened and thickened (D). (E), unaffected contralateral wing of specimen in (D). Scale bar = 1875 μm.

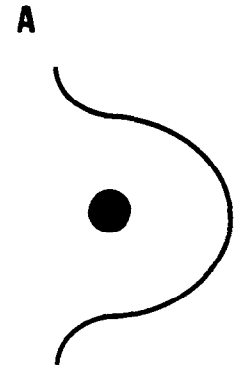
A

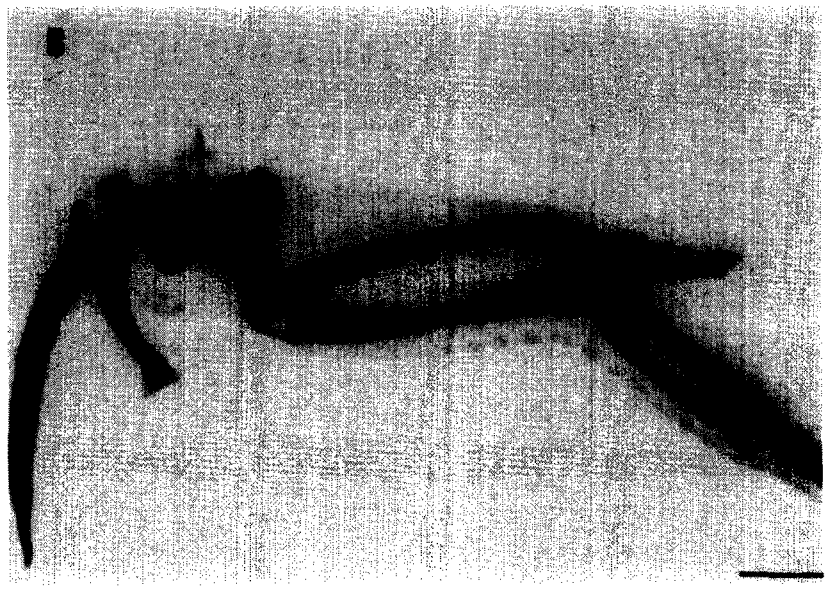
B

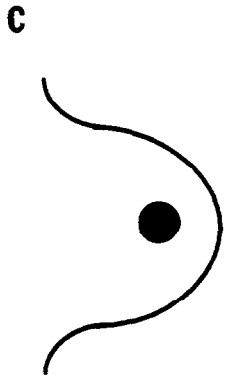
C

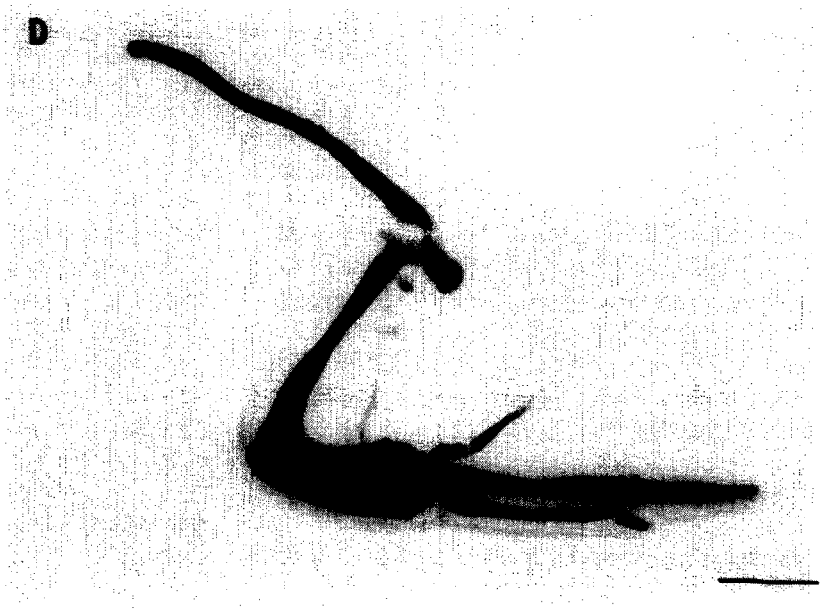
D

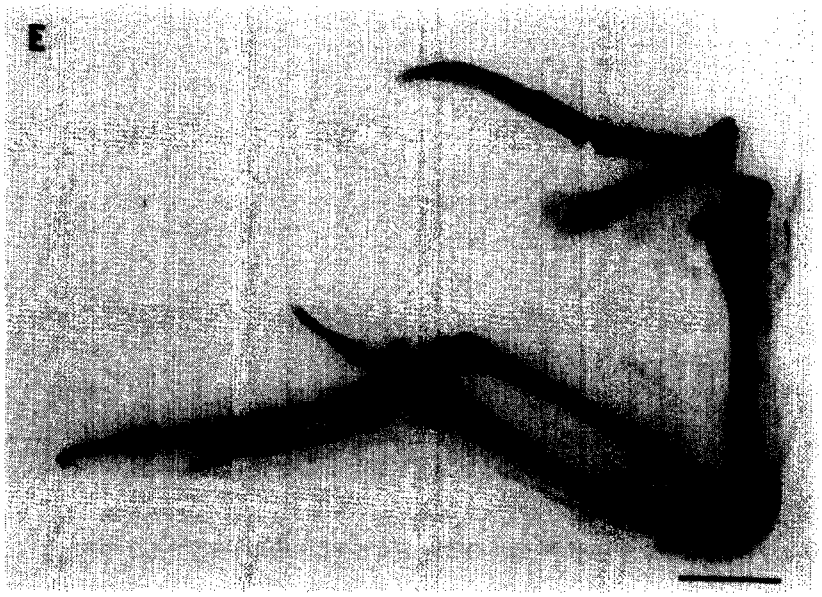
E

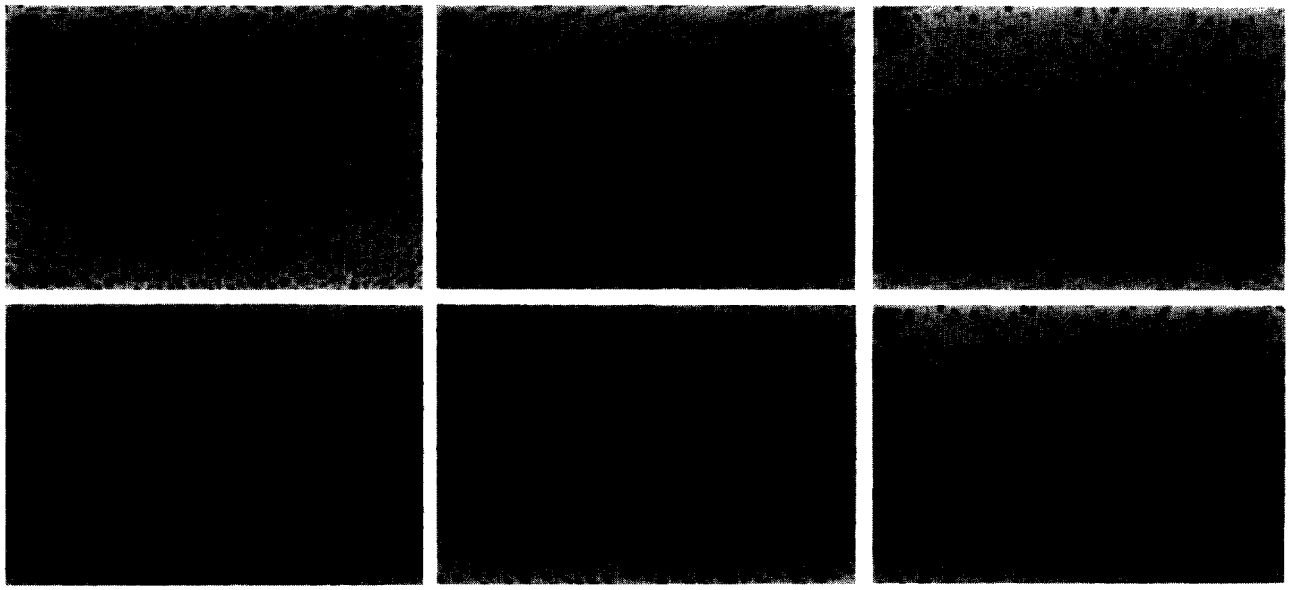

Fig. 7. Morphology of chondrocytes in a control humerus (A–C) and a severely affected humerus from an mBMP-4/RCAS-infected limb (D–F). Normal rounded cell zone (A) and corresponding region at the end of the affected humerus (D). Normal flattened cell zone (B) and corresponding region of the affected humerus (E). Normal hypertrophic zone (C) and corresponding region at the midpoint of the affected humerus (F). In (A), cells are rounded and densely packed; in (B), cells are flattened and ordered; in (C), cells have distinct lacunae. In (D–F), cells show little organisation and do not have the characteristic morphology of the corresponding zones. Scale bar = 50 μm.

genesis, and cells at the margins of the cartilage element were aligned longitudinally and had a denser-staining matrix, suggesting an appositional origin (Fig. 9C). Severely affected limbs showed little osteogenic differentiation on embryonic day 10 (compare Fig. 9A and Fig. 9B). When present, this was often ectopic, being displaced towards the peripheral ectoderm (Fig. 9D).

2.6. *Cell density in affected skeletal elements*

The density of chondrocytes in the rounded, flattened and hypertrophic zones of unaffected control humeri, and in corresponding regions of severely affected humeri was measured. In hBMP-2/RCAS-infected limbs ($n = 2$), cell densities in these regions were 46%, 15% and 24% lower, respectively, than in unaffected limbs. In BMP-4/RCAS-infected limbs ($n = 4$), cell densities were 52%, 20% and 10% lower, respectively, than in unaffected limbs. However, since the volume of the affected elements was at least five times greater than that of the control elements, there were clearly increased numbers of chondrocytes in affected elements.

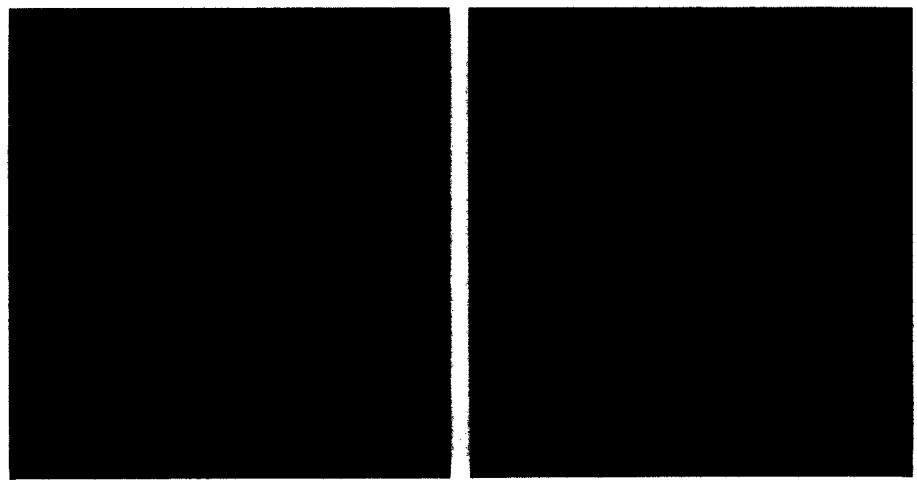

Fig. 8. Expression of type X collagen in control (A) and mBMP-4/RCAS-infected (B) limbs. Type X collagen is visualised by indirect immunofluorescence. Perilacunar immunopositive staining is seen in (A), but not in (B). Scale bar = 50 μm.

2.7. Mitotic activity of chondrocytes in affected skeletal elements

To determine whether the increased number of chondrocytes in affected cartilage elements was due to increased cell proliferation, S-phase chondrocytes were immunolocalised with an antibody against proliferating cell nuclear antigen. The mitotic index in the proximal epiphyseal round cell zone of the humeri of normal stage 27/28 wings was 0.033 ($n = 2$), while in the corresponding region of affected limbs it was 0.025 ($n = 2$). Therefore, BMP overexpression did not appear to alter the mitotic index of affected cells significantly.

3. Discussion

BMPs are well known to induce formation of ectopic bone via an endochondral pathway when implanted into adults. However, in situ hybridization studies and analyses of mouse mutants have suggested that BMPs also have important roles in embryonic skeletal development. We have shown here that *Bmp-2* is expressed in mesenchyme surrounding early cartilage condensations, and that *Bmp-4* is expressed in the perichondrium, a layer of fibroblastic cells surrounding cartilage elements that may be involved in appositional growth of the cartilage, particularly in the epiphyseal regions. Overexpression of BMP-2 or BMP-4, using retroviral vectors, resulted in a dramatic increase in the volume of skeletal elements. In elements showing severe dysplasia, the ordered arrangement of the chondrocytes was abolished, and there was a delay in the terminal differentiation of chondrocytes and in the formation of periosteum, which gives rise to bone.

In normal development, after formation of the cartilage rudiment, growth is achieved in four ways: by hypertrophy of chondrocytes, by increased matrix secretion, by a division of chondrocytes (Rooney et al., 1984), and by appositional growth from perichondrial precursors (Fell and Canti, 1934). In limbs affected by over-expression of hBMP-2 and mBMP-4, hypertrophy was delayed but there was evidence for a small increase in the amount of matrix and a large increase in the number of chondrocytes present in affected elements. This increase in cell number did not seem to result from increased proliferation of chondrocytes, raising the possibility that hBMP-2 and mBMP-4 induced recruitment of cells to form cartilage, either from the perichondrium or from surrounding mesenchyme. Histological sections of affected limbs showed that cells at the margins of the cartilage element were aligned longitudinally and had a denser-staining matrix, suggesting an appositional origin. In addition, the orientation of the matrix partitions was parallel to the long axis of the rudiment, again supporting the notion of perichondrial recruitment (Fell and Canti, 1934). Since the endogenous chicken *Bmp-4* gene is normally expressed in perichondrium, it is possible that BMP-4 is normally involved in recruitment of perichondrial cells to chondrogenic fate. Over-expression of hBMP-2 and mBMP-4 could be stimulating this process. This would explain why hBMP-2 and mBMP-4 over-expression increased the width but not the length of skeletal elements.

It has also been suggested that prior to formation of the perichondrium, initial cartilage condensations may normally increase in size by recruitment of cells from surrounding mesenchyme (Ede, 1977). In adult rats, BMPs recruit cells from surrounding mesenchyme to a chondrogenic fate during formation of BMP-induced ectopic bone (Reddi and Huggins, 1972; Nathanson et al., 1978). The expression of *Bmp-2* in the mesenchyme surrounding early cartilage condensations in normal developing chick limbs would be consistent with a normal role for BMP-2 in controlling recruitment of mesenchymal cells into condensations. Over-expression of hBMP-2 or mBMP-4 could therefore result in increased recruitment of mesenchymal cells into early cartilage condensations.

In our experiments, therefore, the effects of overexpressing hBMP-2 and mBMP-4 could reflect a normal role for BMP-4 in recruiting perichondrial cells and/or a normal role for BMP-2 in recruiting mesenchymal cells. It is not unexpected that mature BMP-2 and BMP-4, which share approximately 92% amino acid sequence identity, should be able to mimic each other's activities.

Over-expression of hBMP-2 or mBMP-4 caused joint fusion. The reasons for this are not clear. However, interzone cells, which are distinct from cartilage chondrocytes, have some of the properties of perichondrium (Craig et al., 1987) and may give rise to established chondrocytes in the presence of hBMP-2 or mBMP-4. Alternatively, overexpression of hBMP-2 or mBMP-4 may prevent formation of the initial joint which arises from the separation of a single cartilage condensation.

Over-expression of hBMP-2 or mBMP-4 delayed formation of the periosteum. Cells which give rise to the periosteum form from the perichondrium. At present it is unclear whether perichondrial and periosteal cells have the same precursors, or whether they arise from different cell lineages. In vitro studies with BMP-2 and TGFβ have shown these members of the TGFβ family can act differentially to induce formation of either chondrogenic or osteoblastic precursors from a mixture of periosteum/perichondrium-derived precursors (Iwasaki et al. 1993, 1994). In those studies, BMP-2 increased formation of bone while TGFβ increased formation of chondrocytes. In our in vivo study we have shown that hBMP-2 and mBMP-4 inhibit periosteal formation but may promote perichondrial chondrogenesis.

Bmp-4 is expressed at a range of sites in the developing embryo and has been shown to be involved in a number of distinct processes, including *Xenopus* mesoderm induction (Dale et al., 1992), mouse tooth induction (Vainio et al., 1993), chick hindbrain patterning (Graham et al., 1994) and chick neural tube patterning (Liem et al., 1995). *Bmp-2* is also expressed at diverse embryonic sites, and has been

implicated in patterning of the chick limb bud (Francis et al., 1994; Laufer et al., 1994). Here we show additional possible roles for BMP-2 and BMP-4 in the embryo, during the formation of skeletal elements.

Mutation studies have suggested that members of the TGFβ family are critical to the formation of developing skeletal elements and that these factors may play specific roles during growth and morphogenesis of the skeleton. However, how these factors control and influence skeletal morphogenesis is not understood. Whilst in vitro studies have shown that BMPs enhance chondrogenesis (Carrington et al., 1991; Chen et al., 1991, 1992; Sampath et al., 1992, 1993; Roark and Greer, 1994), they have not shown a mechanism by which these factors might influence cartilage growth and morphogenesis in vivo. Our study has suggested that in developing cartilage elements, BMP-2 and BMP-4 induce an increase in the volume of skeletal elements by recruiting non-chondrogenic precursors to form cartilage. Thus, local variations in the concentration of BMP-2 and/or BMP-4 may be crucial for determining the shape and size of skeletal elements.

4. Experimental procedures

4.1. Chick embryos

Fertilised wild type chicken eggs (White Leghorn) were obtained from Poyndon Farm, Waltham Cross, Hertfordshire, UK and fertilised 0 line chicken eggs were obtained from the BBSRC Institute for Animal Health, Compton, Berkshire, UK. Eggs were incubated at 38 ± 1°C and embryos staged according to Hamburger and Hamilton (1951).

4.2. In situ hybridisation to whole mounts and tissue sections

Embryos were fixed in 4% (w/v) paraformaldehyde and processed as previously described for in situ hybridization to whole mounts or tissue sections (Francis et al., 1994). In situ hybridisation of digoxigenin-labelled RNA probes to whole mounts, and of ^{35}S-labelled RNA probes to tissue sections was performed as described by Francis-West et al. (1995). Probes for chicken *Bmp-2* or *Bmp-4* transcripts were prepared as described by Francis et al. (1994). Probes for human *Bmp-2* or mouse *Bmp-4* transcripts were pre-

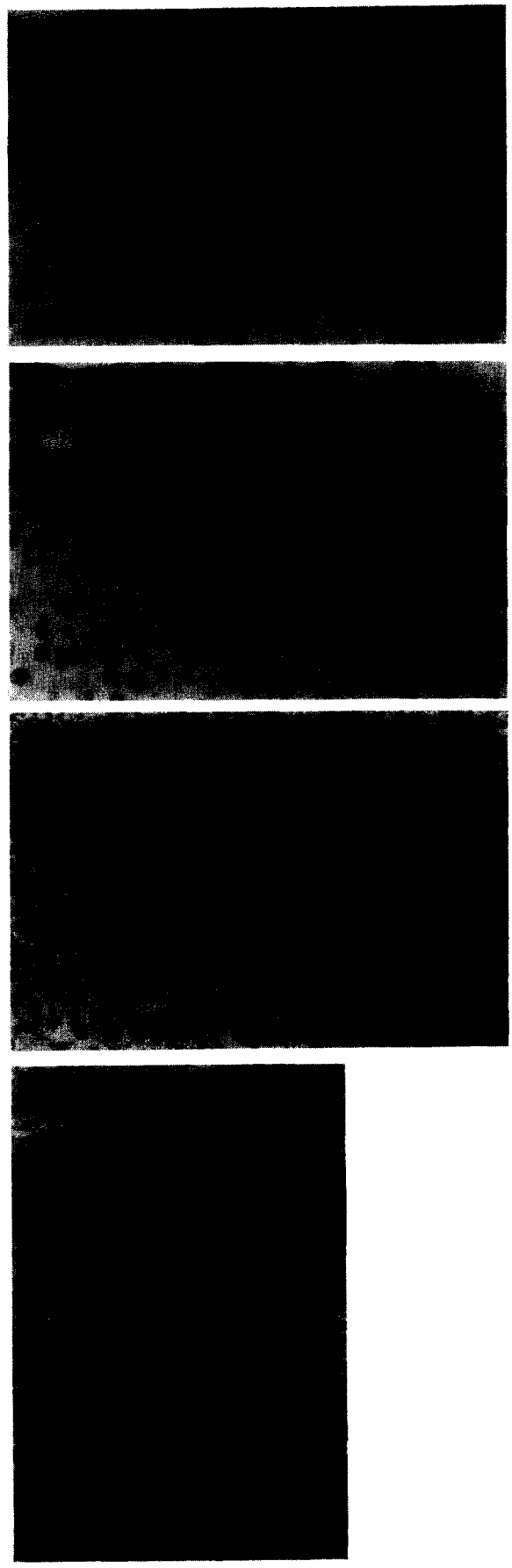

Fig. 9. The chondrial/periosteal structure in the diaphyseal region of the humerus of control (A) and mBMP-4/RCAS-infected (B–D) limbs. In (A), a double layered periosteum has formed (outer fibrous, inner combined), whereas in (B) there is no periosteum and the perichondrium appears disorganised. (C) shows the margin of a cartilage element with a perichondrial-like structure with darker staining matrix partitions (arrowed). (D) shows the presence of ectopic bone, which appears to have been displaced from the cartilage element. Cartilage elements were stained with Mallory's triple stain. B, bone; C, chondrocytes; Pc, perichondrium; Pe, periosteum. Scale bar = 50 μm.

pared as described by Wozney et al. (1988) and Jones et al. (1991), respectively.

4.3. Construction of recombinant retroviral plasmids encoding human BMP-2 or mouse BMP-4

The human BMP-2 (hBMP-2) coding region, and 40 nucleotides of 3′ non-coding region were excised from plasmid PSP65 (Wozney et al., 1988) by digestion with *SalI*, and inserted into the *SalI* site of adaptor plasmid Cla12 (Hughes et al., 1987). Inserted sequences were then excised by digestion with *ClaI* and inserted into the *ClaI* site of replication-defective retroviral vector pCRNCM (de la Pompa and Zeller, 1993) or of replication-competent retroviral vector RCASBP(A) (Hughes et al., 1987). Clones containing the hBMP-2 coding region in the sense orientation (hBMP-2/pCRNCM and hBMP-2/RCAS) or the antisense orientation (Control/pCRNCM and Control-2/RCAS) were selected, the latter for use as negative controls.

To construct a retrovirus encoding BMP-4, the mouse BMP-4 (mBMP-4) coding region was amplified by PCR, using mouse *Bmp-4* cDNA clone mBMP-2b 1321 (Jones et al., 1991) as a template, and using oligonucleotide primers with the sequences CAA GAC ACC ATG **G**TT CCT GG and CGG ATC CTG ATC TCA GCG GCA TC. This introduced a *NcoI* site into the second codon of the BMP-4 coding region by changing the fourth nucleotide of the open reading frame to G (in bold). A *Bam*HI site was added at the 3′ end of the open reading frame. The *NcoI*/*Bam*HI fragment was subcloned into adaptor plasmid Cla12 Nco (Hughes et al., 1987), and the m*Bmp-4* insert was sequenced to ensure that no errors had been introduced during PCR. The *ClaI* fragment containing the m*Bmp-4* insert was then cloned into the *ClaI* site of RCASBP(A) and its orientation determined by nucleotide sequencing and restriction analysis. Clones containing the mBMP-4 coding region in the sense (mBMP-4/RCAS) or antisense (Control-4/RCAS) orientation were selected, the latter for use as a negative control.

4.4. Production of infectious recombinant retrovirus particles

Infectious hBMP-2/pCRNCM and Control/pCRNCM viruses were produced in the quail packaging cell line Q2bn (Stoker and Bissel, 1988). Q2bn cells were grown in 40% (v/v) Dulbecco's modified Eagle's medium (DMEM), 40% (v/v) Ham's F12 medium, 8% (v/v) foetal calf serum, 2% (v/v) chicken serum and were transfected with 10 μg of hBMP-2/pCRNCM or Control/pCRNCM DNA using Transfectam (Promega), according to the manufacturer's instructions. Stable transfectants were selected in G418 and cloned as described by de la Pompa and Zeller (1993). The titre of virus particles produced by each clone was determined as described by de la Pompa and Zeller (1993). The hBMP-2/pCRNCM and Control/pCRNCM clones that produced the highest titres of retrovirus particles (approximately 10^6 ml^{-1}) were chosen for grafting into chick limb buds.

Infectious hBMP-2/RCAS, mBMP-4/RCAS, Control-2/RCAS and Control-4/RCAS viruses were produced in 0 line chick embryo fibroblasts (CEF). CEF were isolated from 10 day 0 line embryos and grown in DMEM containing 10% (v/v) foetal calf serum. CEF were transfected with 10 μg of retroviral construct DNA by calcium phosphate precipitation, as described by Morgan et al. (1992). The extent of viral infection in cultures was determined by staining with monoclonal anti-GAG antibody 3C2 (Potts et al., 1987). When all cells stained positive, they were prepared for grafting into limb buds.

4.5. Grafting of retrovirus-infected cells into chick limb buds

Infected cells for grafting were prepared as described by Riddle et al. (1993), except that cells were not stained with Nile blue sulphate and were left to consolidate for 1 h at 37°C. Pellets of infected cells, approximately 200 μm^3 in size, were grafted into right wing buds of White Leghorn embryos at various stages of development. Embryos were harvested and processed for in situ hybridisation to whole mounts or tissue sections. After whole mount in situ hybridisation, some embryos were stained with alcian green and cleared in methyl salicylate to determine cartilage morphology and to correlate this with viral spread. For histological examination, whole mounts were embedded in wax, sectioned at 8 μm and stained with Mallory's triple stain or haematoxylin and eosin.

4.6. Northern blotting and hybridization

Polyadenylated RNA was isolated from virus-infected CEF, blotted and hybridised with a ^{32}P-labelled RNA probe for mouse *Bmp-4* RNA (Jones et al., 1991) as previously described (Francis et al., 1994).

4.7. Localisation of S-phase cells

Virus-infected cells were grafted to chick limb buds at stage 18/19. Embryos were fixed 72 h later, at stage 27/28, processed into wax and sectioned at 7 μm. Sections were de-waxed in xylene for 10 min, with two changes of xylene, rehydrated through a descending series of alcohols (5 min each step) to PBS, washed in three changes of PBS (5 min each wash) and blocked by incubating in 6% (w/v) BSA in PBS for 5 min. PC10 (anti-human proliferation cell nuclear antigen, DAKO; 0.25 mg/ml IgG) was applied for 30 min. Sections were washed three times for a total of 15 min in PBS and then incubated in secondary antibody (5 nM gold-conjugated goat anti-mouse IgG; Bioclin, Cardiff) for 45 min. Sections were washed twice for 5 min each with PBS, and the secondary antibody was cross-

linked to sections with 1% (w/v) glutaraldehyde in PBS for 5 min. Sections were washed three times with 'Analar' water (BDH) (5 min each wash) followed by three short washes with 0.75 M Tris–acetate buffer (pH 7.5). Sections were subjected to silver enhancement reagents according to the manufacturer's instructions (Bioclin, Cardiff) and the reaction monitored under a microscope for 15–20 min. Sections were washed in distilled water (two changes, 5 min each), and stained with Harris' haematoxylin and eosin. Control sections were treated with non-immune mouse IgG (primary control) and the secondary antibody was substituted with 1% (w/v) BSA (secondary silver control).

4.8. Immunolocalisation of type X collagen

To localise hypertrophic chondrocytes, a monoclonal antibody (MA3) against chicken type X collagen (Kwan et al., 1989) was used on sections from specimens fixed for in situ hybridisation. Processing up to primary antibody application was as described for proliferating cells above with the exception that after rehydration, sections were subjected to hyaluronidase/chondroitinase digestion (2.5 and 3 U ml^{-1}, respectively, in PBS, pH 7.4) for 45 min at 37°C. Primary antibody application (45 min at room temperature) was followed by routine secondary detection with a fluorescently conjugated rabbit anti-mouse IgG (1:40 dilution; 45 min at room temperature; Sigma). Sections were mounted and photographed on a Zeiss photomicroscope III with fluorescent attachment.

Acknowledgements

We thank Stephen Hughes and Cliff Tabin for the gift of Cla12Nco and RCASBP(A), respectively, Rolf Zeller and Achim Leutz for the gift of pCRNCM, Elizabeth Wang of Genetics Institute for the gift of PSP65 and the monoclonal antibody against human BMP-2, Brigid Hogan for the gift of mouse *Bmp-4* cDNA clones, and A. Kwan for the gift of the antibody against type X collagen. We thank H. Morrison for performing PCNA localisations, Les Dale for performing *Xenopus* animal cap assays and A. Grigoriadis for critically reading the manuscript. This work was supported by grants from the Biotechnology and Biological Sciences Research Council, the Medical Research Council, the European Commission and the Arthritis and Rheumatism Council.

References

Bowen, J., Hinchliffe, J.R., Horder, P. and Reeve, A.M. (1989) Anat. Embryol. 179, 269–283.

Carrington, J.L., Chen, P., Yanagishita, M. and Reddi, A.H. (1991) Dev. Biol. 146, 406–415.

Chang, S.C., Hoang, B., Thomas, J.T., Vukicevi, S., Luyten, F.P., Ryba, N.J.P., Kazak, C.A., Reddi, A.H. and Moos, M. (1994) J. Biol. Chem. 269, 1–8.

Chen, P., Carrington, J.L., Hammonds, R.G. and Reddi, A.H. (1991) Exp. Cell Res. 195, 509–515.

Chen, P., Carrington, J.L., Paralkar, V.M., Pierce, G.F. and Reddi, A.H. (1992) Exp. Cell Res. 200, 110–117.

Craig, F.M., Bentley, G. and Archer, C.W. (1987) Development 99, 383–391.

Dale, L., Howes, G., Price, B.M.J. and Smith, J.C. (1992) Development 115, 573–585.

de la Pompa, J.L. and Zeller, R. (1993) Mech. Dev. 43, 187–198.

Ede, D.A., Flint, O.P., Wilby, O.K. and Colquhoun, P. (1977) In D.D. Ede, J.A. Hinchliffe and M. Balls (eds.), Vertebrate Limb and Somite Morphogenesis, Cambridge University Press, Cambridge, pp. 61–79.

Fell, H.B. and Canti, R.G. (1934) Proc. R. Soc. 116, 316–351.

Francis, P.H., Richardson, M.K., Brickell, P.M. and Tickle, C. (1994) Development 120, 209–218.

Francis-West, P.H., Robertson, K., Ede, D.A., Rodriguez, C., Izpisúa-Belmonte, J.-C., Houston, B., Burt, D.W., Gribbin, C. Brickell, P.M. and Tickle, C. (1995) Dev. Dyn. 203, 187–197.

Graham, A., Francis-West, P., Brickell, P. and Lumsden, A. (1994) Nature 372, 684–686.

Hamburger, V. and Hamilton, H.L. (1951) J. Morphol. 88, 49–92.

Hughes, S.H., Greenhouse, J.J., Petropoulos, C.J. and Sutrave, P. (1987) J. Virol. 61, 3004–3012.

Iwasaki, M., Nakata, K., Nakahara, H., Nakase, T., Kinura, T., Kimata, K., Caplan, A.I. and Ono, K. (1993) Endocrinology 132, 1603–1608.

Iwasaki, M., Nakahara, H., Nakase, T., Kimura, T., Takaoka, K., Caplan, A.I. and Ono, K. (1994) J. Bone Mineral Res. 9, 1195–1204.

Jones, C.M., Lyons, K.M. and Hogan, B.L.M. (1991) Development 111, 531–542.

Kingsley, D.M., Bland, A.E., Grubber, J.M., Marker, P.C., Russell, L.B., Copeland, N.G. and Jenkins, N.A. (1992) Cell 71, 399–410.

Kingsley, D.M. (1994) Trends Genet. 10, 16–21.

Kwan, A.P., Dickson, I., Freemont, A. and Grant, M.E. (1989) J. Cell Biol. 109, 1849–1856.

Laufer, E., Nelson, C.E., Johnson, R.L., Morgan, B.A. and Tabin, C. (1994) Cell 79, 993–1003.

Liem, K.F., Tremml, G., Roelink, H. and Jessell, T.M. (1995) Cell 82, 969–979.

Lyons, K.M., Pelton, R.W. and Hogan, B.L.M. (1989) Genes Dev. 3, 1657–1668.

Morgan, B.A., Izpisúa-Belmonte, J.-C., Duboule, D. and Tabin, C.J. (1992) Nature 358, 236–239.

Nathanson, M.A., Hilfer, S.R. and Searls, R.L. (1978) Dev. Biol. 64, 99–117.

Potts, W.M., Olsen, M., Boettinger, D. and Vogt, V.M. (1987) J. Gen. Virol. 68, 3177–3182.

Reddi, A.H. and Huggins, C. (1972) Proc. Natl. Acad. Sci. USA 69, 1601–1605.

Riddle, R.D., Johnson, R.L., Laufer, E. and Tabin, C. (1993) Cell 75, 1401–1416.

Roark, E.F. and Greer, K. (1994) Dev. Dyn. 200, 103–116.

Rooney, P., Archer, C. and Wolpert, L. (1984) In R. Trelstad (ed.), The Role of Extracellular Matrix in Development, Wiley-Liss, New York, pp. 305–322.

Rooney, P. and Archer, C.W. (1992) J. Anat. 181, 393–401.

Sampath, T.K., Maliakal, J.C., Hauschka, P.V., Jones, W.K., Sasak, H., Tucker, R.F., White, K.H., Coughlin, J.E., Tucker, M.M., Pang, R.H.L., Corbett, C., Ozkaynak, E., Oppermann, H. and Rueger, D.C. (1992) J. Biol. Chem. 267, 20352–20362.

Sampath, T.K., Rashka, K.E., Doctor, J.S., Tucker, R.F. and Hoffmann, F.M. (1993) Proc. Natl. Acad. Sci. USA 90, 6004–6008.

Saunders, J.W. (1948) J. Exp. Zool. 108, 363–404.

Stoker, A.W. and Bissel, M. (1988) J. Virol. 3, 1008–1015.

Storm, E.E., Huynh, T.V., Copeland, N.G., Jenkins, N.A., Kingsley, D.M. and Lee, S.-J. (1994) Nature 368, 639–643.

Thorogood, P. (1983) In B.K. Hall (ed.), Cartilage, Academic Press, San Diego, CA, pp. 223–254.

Vainio, S., Karavanova, I., Jowett, A. and Thesleff, I. (1993) Cell 75, 45–58.

Wolpert, L. and Tickle, C. (1993) In M. Bernfield (ed.), Molecular Basis of Morphogenesis, Wiley-Liss, New York, pp. 207–219.

Wozney, J.M., Rosen, V., Celeste, A.J., Mitsock, L.M., Whitters, M.J., Kriz, R.W., Hewick, R.M. and Wang, E.A. (1988) Science 242, 1528–1534.

Wozney, J.M., Capparella, J. and Rosen, V. (1993) In M. Bernfield (ed.), Molecular Basis of Morphogenesis, Wiley-Liss, New York, pp. 221–230.